Basic Semiconductor Physics

II	III	IV	V	VI
4 9.012 Be beryllium	5 10.81 B boron	6 12.01 C carbon	7 14.01 N nitrogen	8 16.00 O oxygen
12 24.30 Mg magnesium	13 26.98 Al aluminum	14 28.09 Si silicon	15 30.97 P phosphorus	16 32.06 S sulfur
30 65.38 Zn zinc	31 69.72 Ga gallium	32 72.59 Ge germanium	33 74.92 As arsenic	34 78.96 Se selenium
48 65.38 Cd cadmium	49 69.72 In indium	50 72.59 Sn tin	51 74.92 Sb antimony	52 78.96 Te tellurium
80 200.6 Hg mercury	81 204.4 Tl thallium	82 207.2 Pb lead	83 209.0 Bi bismuth	84 210.0 Po polonium

Figure 1.1. Portion of the Periodic Table showing elements that combine into semiconductors. Each entry consists of the name of the element, its chemical symbol, atomic number, and mass. Columns of the Table are indicated by roman numerals.

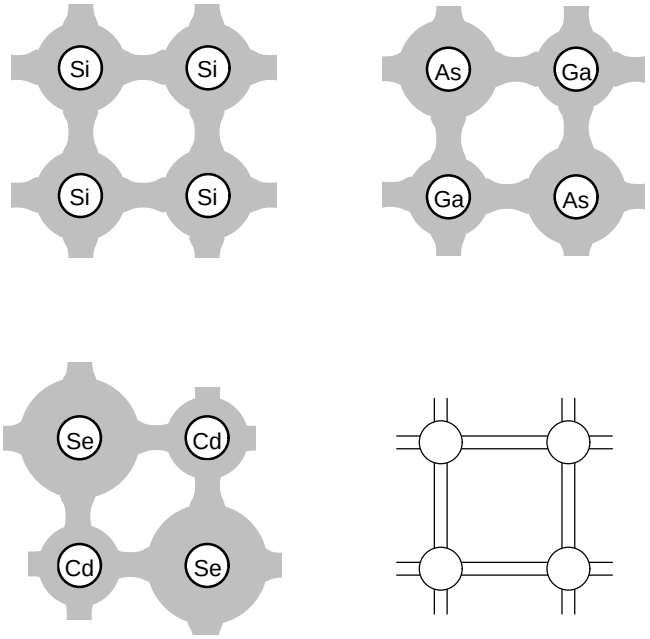

Figure 1.2. Charge distribution in covalent crystals. Elemental semiconductors (Si, Ge) are *perfectly covalent*; by symmetry electrons shared between two atoms are to be found with equal probability on each atom. Compound semiconductors always have some degree of *ionicity*. In III-V compounds, e.g., GaAs, the five-valent As atom retains slightly more charge than is necessary to compensate for the positive charge of the As^{5+} ion core, while the charge on the Ga^{3+} ion is not entirely compensated. Sharing of electrons occurs still less fairly between the ions Cd^{2+} and Se^{6+} in the II-VI compound CdSe.

The covalent bond picture is reasonably good for all semiconductors. For illustrative purpose it is often convenient to represent the bonding network by circles (ions) and lines (shared electrons). It should be noted of course that the network is 3-dimensional. For most semiconductors each atom indeed has 4 nearest neighbors, as illustrated, but these are located not in the same plane but at the vertices of a tetrahedron, see Fig. 1.3 below.

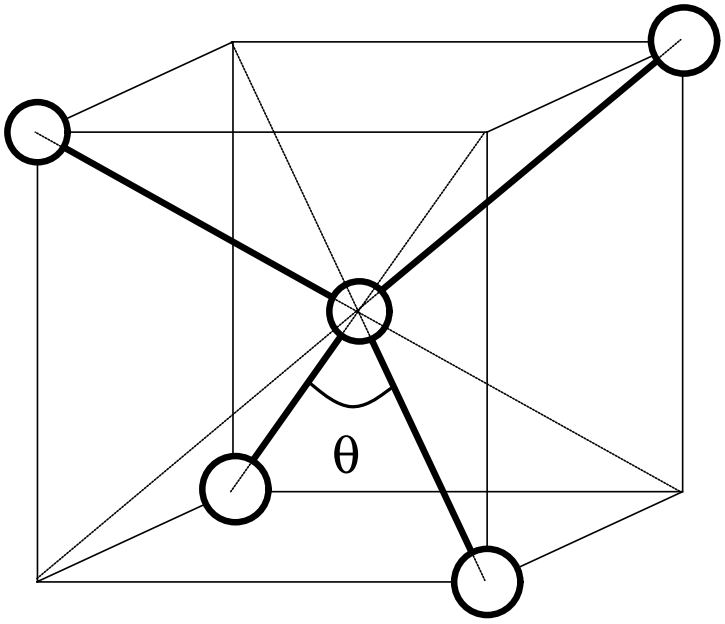

Figure 1.3. Tetrahedral arrangement of atoms in a diamond or zincblende structure. The bonds are along the cube diagonals and the bond angle θ is given by $\cos\theta = -1/3$. Four atoms in the corners define a regular tetrahedron. In a zincblende structure these four are different from the central atom, in the diamond structure they are all the same.

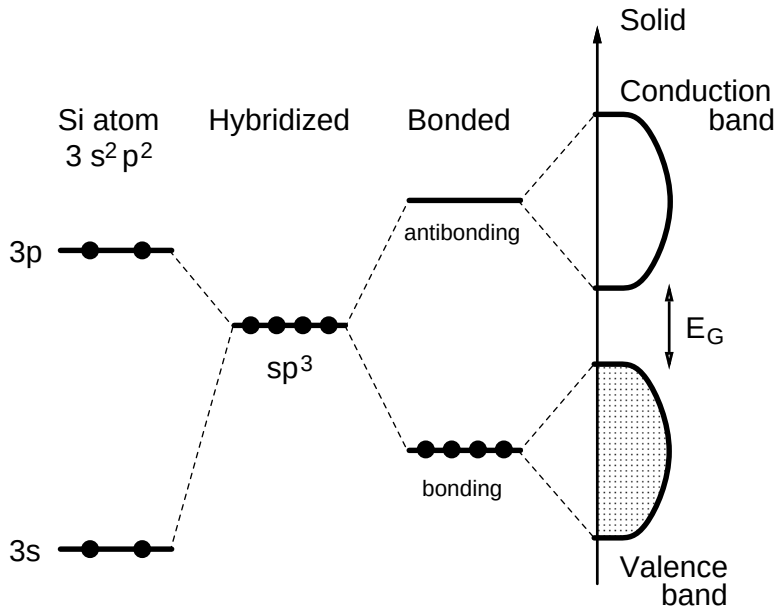

Figure 1.4. Electronic energy levels involved in the covalent bonding scheme. Separation between the 3*p* and 3*s* atomic orbitals is about $6\,eV$. Mixing of these orbitals into 4 equivalent sp^3 hybrids requires promotion of one *s* electron. Separation between the bonding and the antibonding levels ("bare" bandgap) is about $5\,eV$, which is also the "average" separation between the valence and conduction band states. The minimum separation between these bands (the bandgap E_G) in Si is about $1.2\,eV$ at zero temperature.

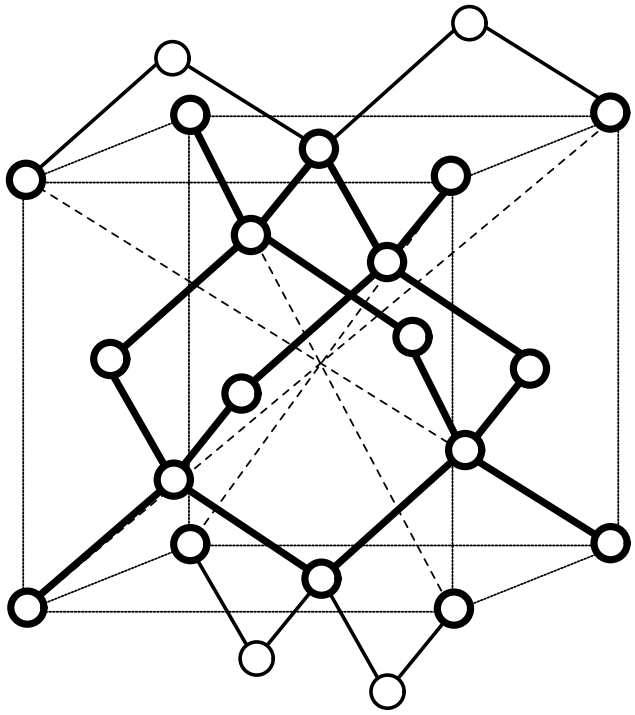

Figure 1.5. The diamond structure, characteristic of Column-IV semiconductors: C (diamond), Si, Ge, α-Sn (grey tin). It is not a Bravais lattice and has two atoms per unit cell. In Cartesian coordinates with axes along the side of a cube of side a the second atom is displaced by a vector $(a/4, a/4, a/4)$ relative to the first. The two-atom unit itself (the basis) is repeated periodically, forming a face-centered cubic (fcc) lattice. The structure can be viewed as two interpenetrating fcc sublattices. There is a *center of inversion* symmetry, located halfway on the line between the two basis atoms. The two fcc sublattices are fully interchanged by the inversion operation, so all atoms in the diamond structure are *symmetry equivalent*. This, however, does not make diamond a Bravais lattice, because there is no way to choose a set of three translation vectors that would generate the entire structure from a single atom.

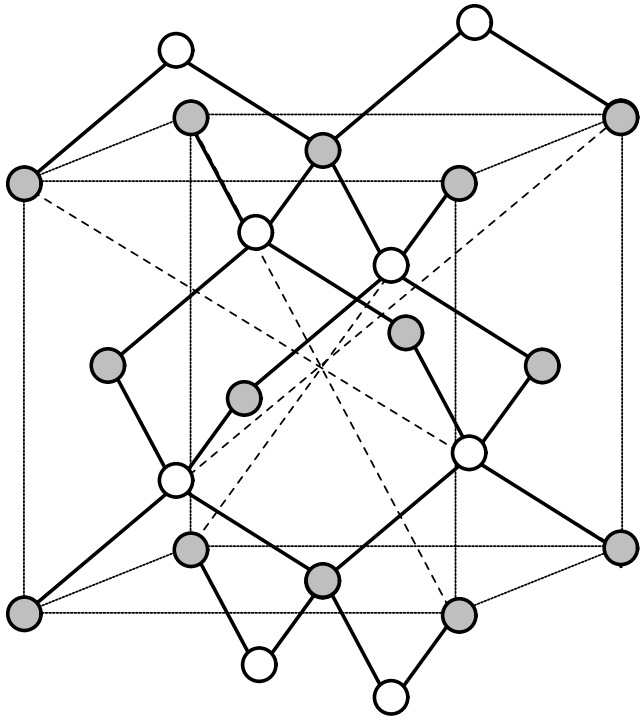

Figure 1.6. The zincblende structure, e.g., GaAs. The figure is similar to Fig. 1.5 except that atoms in alternate planes are colored differently. Gallium atoms form a face centered cubic lattice. An identical sublattice – but shifted along the body diagonal of the cube 1/4th of its length – is formed by atoms of As. Unlike diamond, the zincblende structure does not have an inversion symmetry. Volume a^3 of cube shown is four times the primitive unit cell volume v_c. The number of atoms per unit volume of the crystal is thus $8/a^3$.

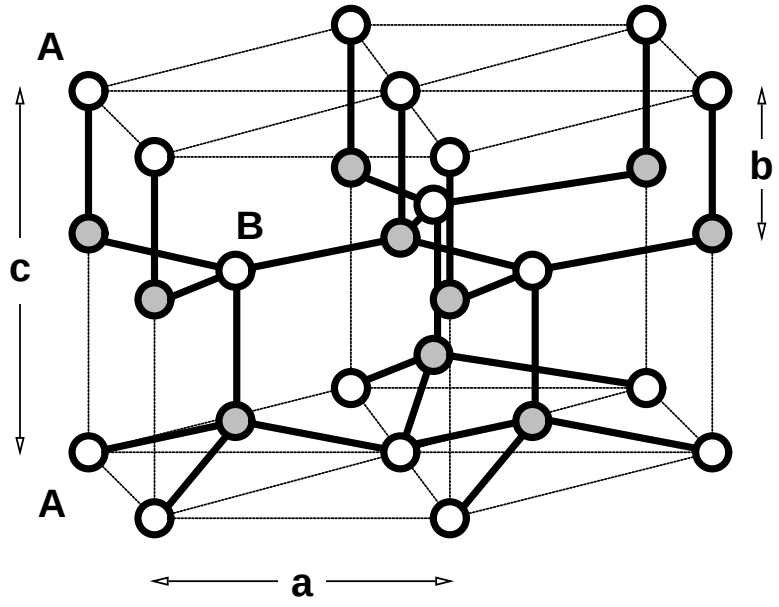

Figure 1.7. The wurtzite structure, e.g., CdSe. Cadmium atoms form a hexagonal lattice with two atoms per unit cell. The second plane of Cd atoms (B) is located exactly in the middle between the two planes of A atoms. The B plane has the same 2-dimensional hexagonal arrangement of atoms as the A plane but is shifted laterally. Position of the B atom relative to A is $\mathbf{a}_1/3 + \mathbf{a}_2/3 + \mathbf{a}_3/2$.

Distance between in-plane A neighbors is denoted by a and the vertical A-A distance by c. Selenium atoms are displaced from cadmium atoms by a distance b in the direction of the hexagonal axis. Thus a general wurtzite structure is described by 3 parameters: the lattice constant a and two dimensionless parameters $\gamma = c/a$ and $\mu = b/a$.

Most wurtzite semiconductors are characterized by the "ideal" values $\gamma = (8/3)^{1/2}$ (hexagonal close packed lattice) and $\mu = (3/8)^{1/2}$ (all bonds are equal). This structure obtains when built with undistorted tetrahedral blocks (Fig. 1.3). Like in the zincblende structure, only atoms of opposite kind are bonded.

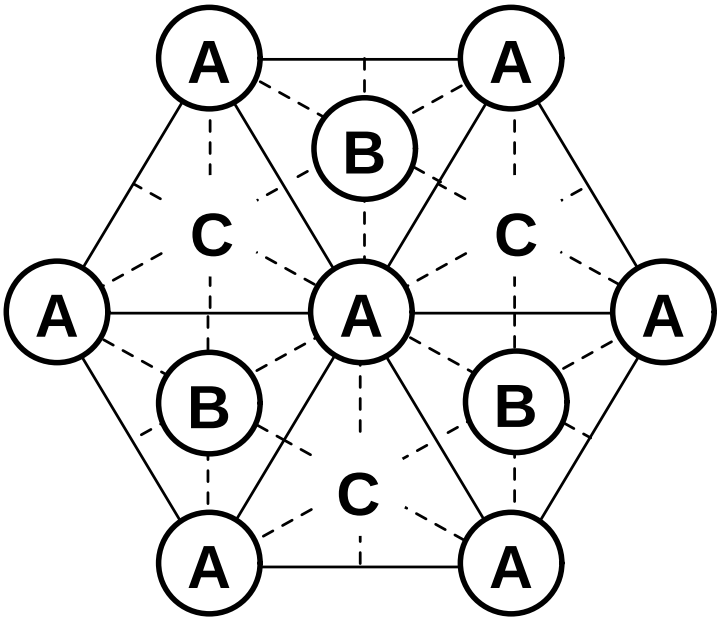

Figure 1.8. The wurtzite structure viewed along the hexagonal axis. Atoms of type B project in the middle of three (out of six) equilateral triangles formed by atoms A. Note that both A and B correspond to the same atomic species (e.g. Cd) and *together* form a hexagonal close packed lattice. (Atoms of Se form another hcp lattice displaced into the page approximately by 3/8 of the distance *c* between two A planes.)

Imagine expanding the spheres A so that they touch in the plane ("close packing"). It is clear that stacking similar spheres on the next level, we cannot fill both B and C positions (distance BC is too short). However, when we go to the next level again, we are free to fill either the three A positions (as is appropriate for hcp lattice) or the three C positions (the latter arrangement corresponds to fcc lattice). Adding a similar sublattice of the second atomic species we obtain either the wurtzite or the diamond structure. Note that while hcp and fcc correspond to a dense packing of spheres, wurtzite and diamond are very loose.

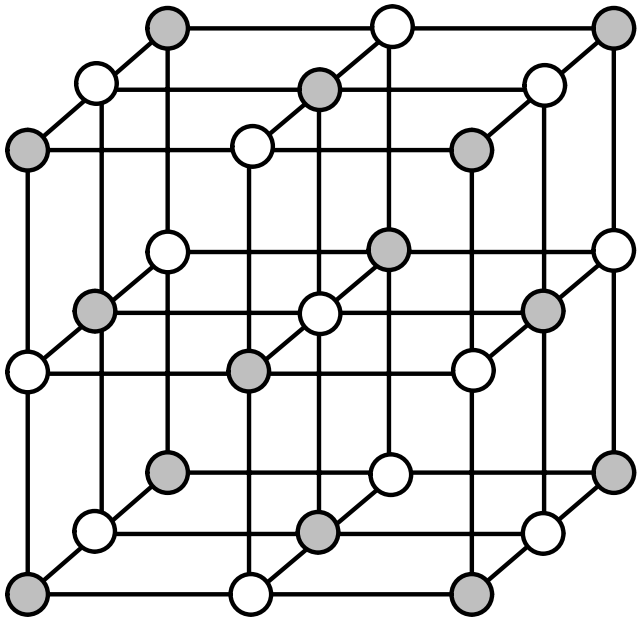

Figure 1.9. The rocksalt (sodium chloride) structure. Some of the IV-VI semiconductors (mainly the lead-salt family: PbS, PbSe, PbTe) crystallize as rocksalt. This structure is *octahedrally* coordinated ($z = 6$). Atoms (or ions) of Pb and S occupy alternate sites of a simple cubic lattice in such a way that each atom has six nearest neighbors of the other kind. Like the zincblende, the rocksalt structure is face-centered cubic with a two-atom basis and has $8/a^3$ atoms per unit volume. Note that the shaded "atoms" are positioned in the same way as in Fig. 1.6 – exhibiting the face-centered arrangement. The white and the shaded "atoms" form two interpenetrating fcc sublattices.

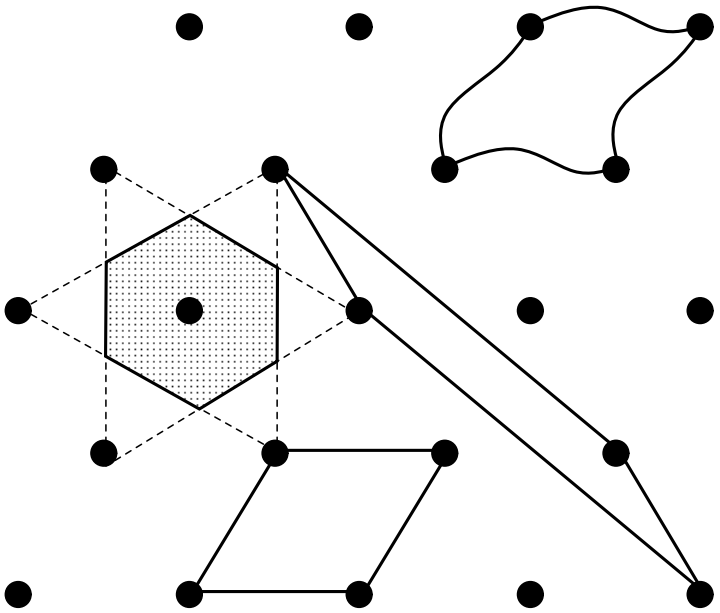

Figure 1.10. Primitive unit cells of a honeycomb lattice. Any parallelogram formed by four lattice points as vertices will serve, provided no other lattice point falls on its boundary or inside. Boundaries of the cell do not have to be made of straight lines: the opposite sides may be replaced by a pair of congruent curves. All primitive cells have the same area.

The shaded hexagon represents the Wigner-Seitz primitive cell. Note its symmetry (point symmetry of the honeycomb lattice) and observe the scaffolding used for its construction. Lines were drawn from the central point to its neighbors (in this case only nearest neighbors were sufficient, but in general several shells of neighbors may be required) and each line was bisected with a perpendicular line.

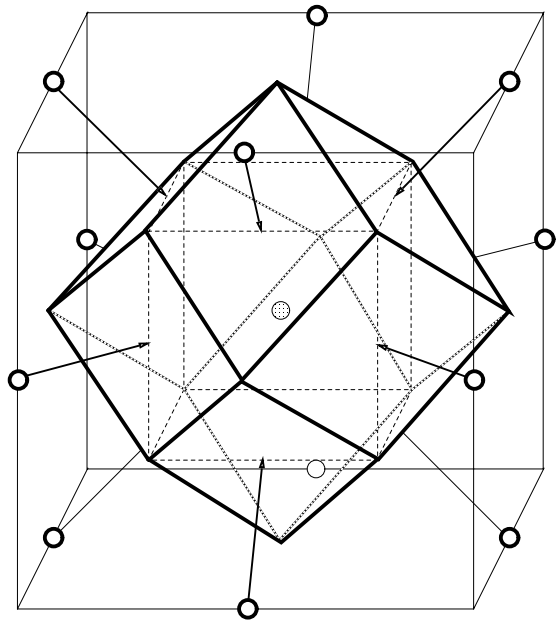

Figure 1.11. Wigner-Seitz cell for the face-centered cubic lattice, a rhombic dodecahedron of volume $v_c = a^3/4$. It has 14 vertices, 24 edges and 12 faces. Faces of the cell are twelve equal rhombi. The vertices are not all equivalent: the six that touch the face centers of the big cube are common to four rhombi, while the other eight vertices are common to three rhombi. Observe and contemplate the cell symmetry. In diamond, zincblende, and rocksalt structures the primitive cell accommodates two atoms.

Exercise: Construct the fcc Wigner-Seitz cell geometrically. Start from the fcc lattice of white "atoms" in Fig. 1.9 (conveniently, it has one site at the center of the cube). Draw a small cube (edge $a/2$) around the central atom, as shown by the dashed line in Fig. 1.11. Make replicas of the small cube (like a three-dimensional chessboard). Use the body diagonals of the replica cubes to identify 6 pyramids – each covering one face of the central cube. These pyramids together with the central cube form the rhombic dodecahedron. Six vertices of the dodecahedron (those that coincide with the apices of pyramids) belong to four edges each, the other eight vertices (coinciding with the small cube corners) are intersections of three edges.

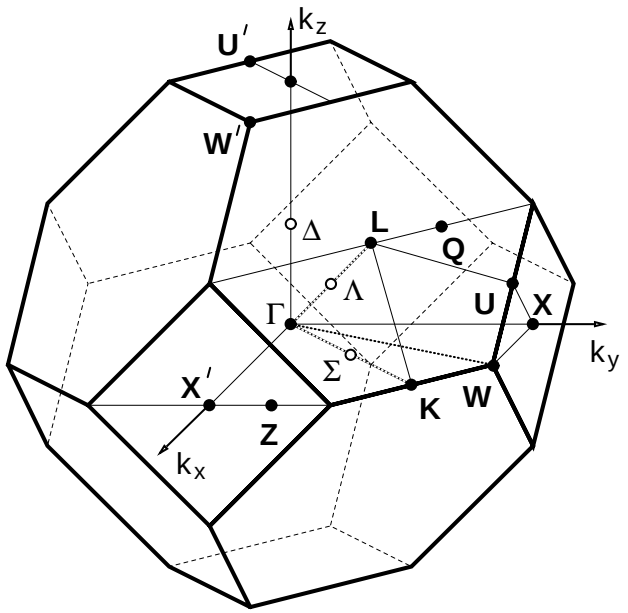

Figure 1.12. The first Brillouin zone of the face centered cubic lattice, a "truncated octahedron" of volume $4(2\pi/a)^3$. It has 14 faces: six squares along the <100> directions and eight regular hexagons along the <111> directions. Symmetry points are labeled conventionally (without the primes). Note that points K and U′ are *identical* (different by a reciprocal lattice vector) and so are points W and W′ – but not X and X′. The number of electronic states (including spin) in the Brillouin zone is $8/a^3$ per unit volume.

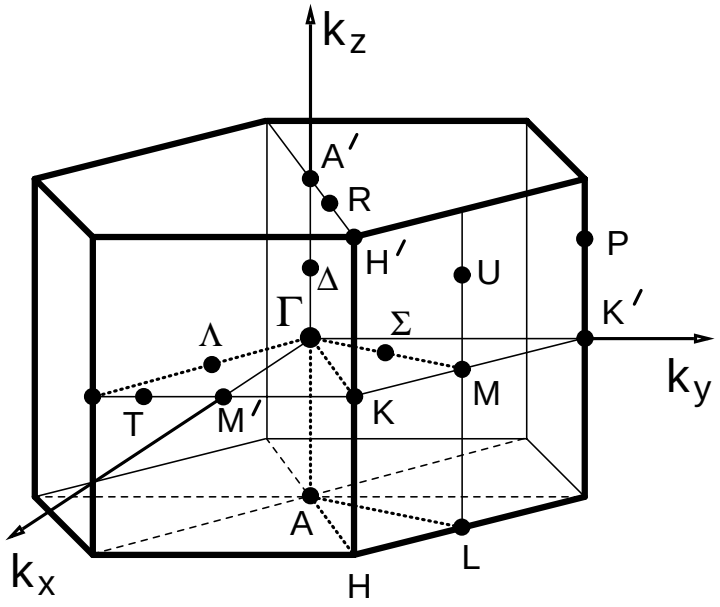

Figure 1.13. The first Brillouin zone of a hexagonal lattice, showing the symmetry points and symmetry axes. It is a hexagonal prism of volume 0.ds 0 √ $(2\pi)^3/v_c$, where $v_c = a^2c/2$ is the volume of a similar prism corresponding to the Wigner-Seitz cell. These two prisms are rotated by 30° with respect to one another. The number of electronic states (including spin) 0.ds 0 √ in the Brillouin zone is $4/(a^2c)$ per unit volume.

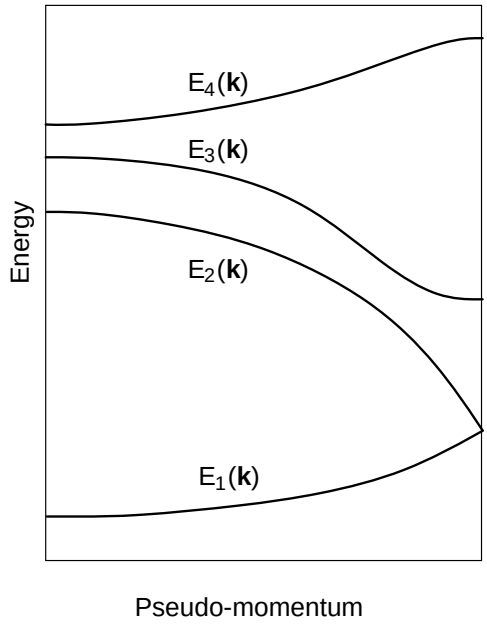

Figure 1.14. Illustration of how different bands may be arranged with respect to one another. Overlap of two bands (like E_2 and E_3) does not imply their intersection or touching. Coincidences of energies between pairs of points in these bands is an example of accidental degeneracy. Bands E_1 and E_2 touch at a point, whose symmetry is the likely cause of this degeneracy. Energy gap separates bands E_3 and E_4.

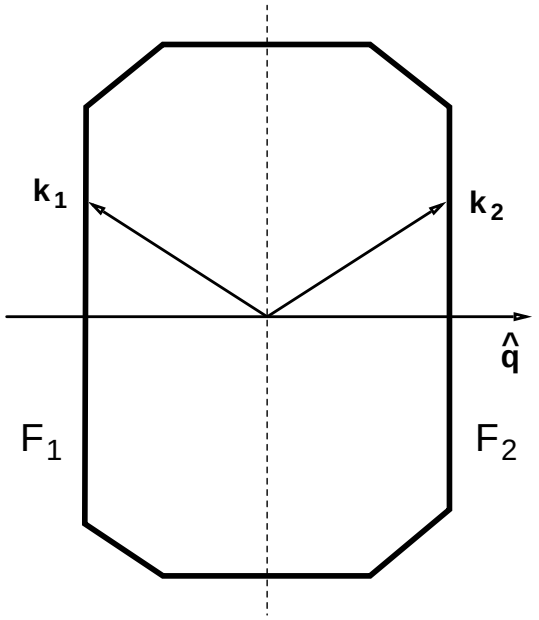

Figure 1.15. Schematic cross-section of a Brillouin zone in the plane normal to a crystal symmetry plane (shown by the dashed line). Faces F_1 and F_2 are parallel to the symmetry plane and perpendicular to a direction $\hat{\mathbf{q}}$. Opposite faces of the Brillouin zone are identical (symbolically, $F_1 = F_2 \equiv F$). Therefore, symmetry related points $\mathbf{k}_1$ and $\mathbf{k}_2$ represent the same crystal momentum. For every energy band $E_n(\mathbf{k})$, its normal derivative vanishes on the entire area of the polygon F.

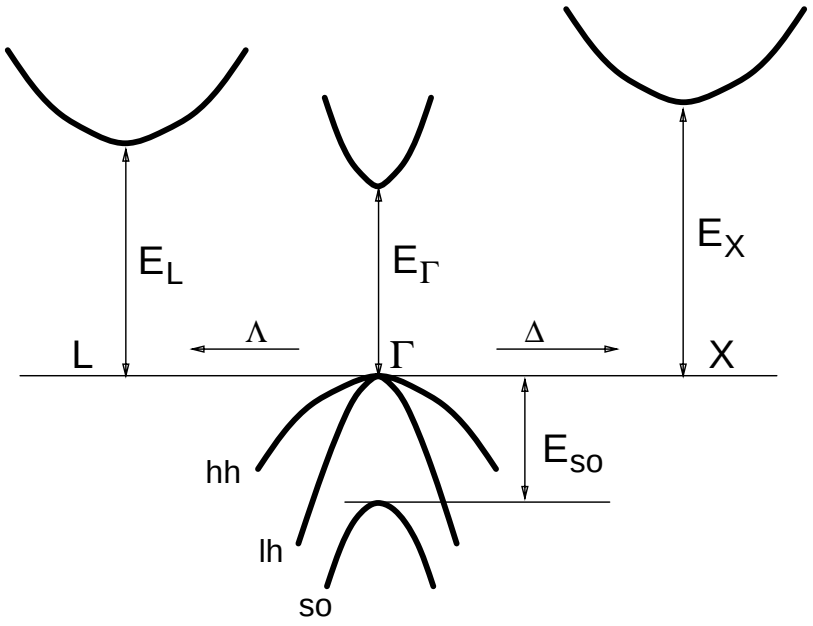

Figure 1.16. Important extremal points in the band structure of cubic semiconductors. The schematic picture (drawn not to scale) is appropriate for a direct-gap III-V semiconductor. For GaAs at room temperature the indicated energies are:

$E_\Gamma = 1.42\,eV$, $E_\mathrm{L} = 1.71\,eV$, $E_\mathrm{X} = 1.90\,eV$, $E_\mathrm{so} = 0.34\,eV$.

In silicon the lowest conduction band point is in the Δ direction, 85% of the way to X point. The indicated energies for silicon at 300 K are:

$E_\Gamma = 4.08\,eV$, $E_\mathrm{L} = 1.87\,eV$, $E_\Delta = 1.13\,eV$, $E_\mathrm{so} = 0.04\,eV$.

In Ge the lowest conduction band point is at L but the Γ point is not far away:

$E_\Gamma = 0.89\,eV$, $E_\mathrm{L} = 0.76\,eV$, $E_\Delta = 0.96\,eV$, $E_\mathrm{so} = 0.29\,eV$.

Additional band structure data can be found in Tables at the end of the book.

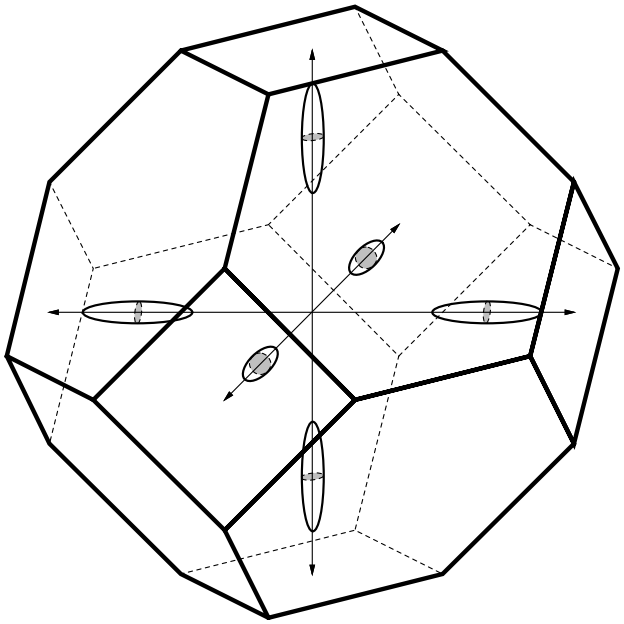

Figure 1.17. Surface of constant energy in the vicinity of the conduction band edge in silicon represents six ellipsoids of revolution, extended along <100> directions. The band curvature is least in the longitudinal direction (heavy mass) and highest in the transverse direction (light mass) The effective mass ratio $m_l/m_t \approx 5$.

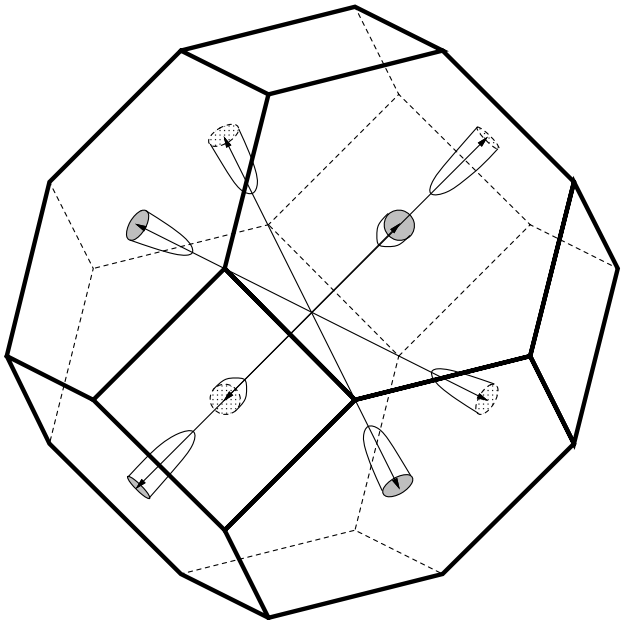

Figure 1.18. Surface of constant energy in the vicinity of the conduction band edge in germanium represents four ellipsoids of revolution, extended along <111> directions. The effective mass ratio is very large, $m_l/m_t = 20$, so that each ellipsoid really looks like a sausage.

In order to exhibit a full ellipsoid we would have to chose a primitive cell for which some L point would be internal. In the Brillouin zone picture, each ellipsoid is cut in two by the boundary and the equivalent half is shifted to the opposite face by a reciprocal lattice vector.

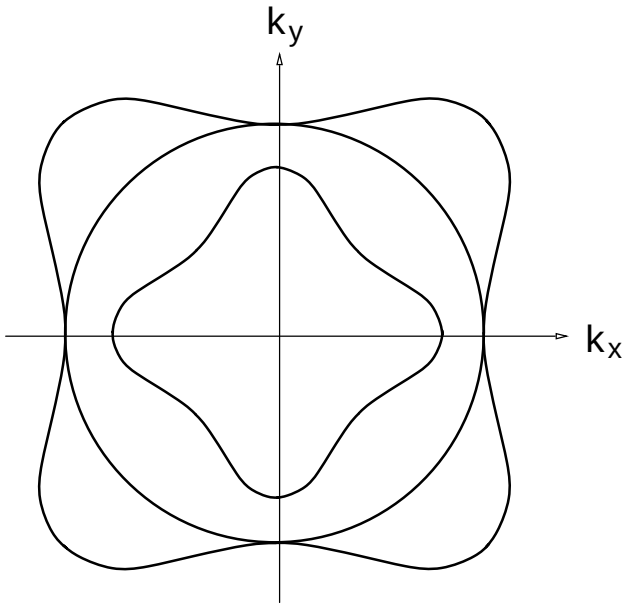

Figure 1.19. Projection on the (001) plane of a constant-energy surface in the vicinity of the three-fold degenerate valence band edge in diamond-structure semiconductors. Three-dimensional surfaces of constant energy are warped spheres. The warping in the figure is much exaggerated.

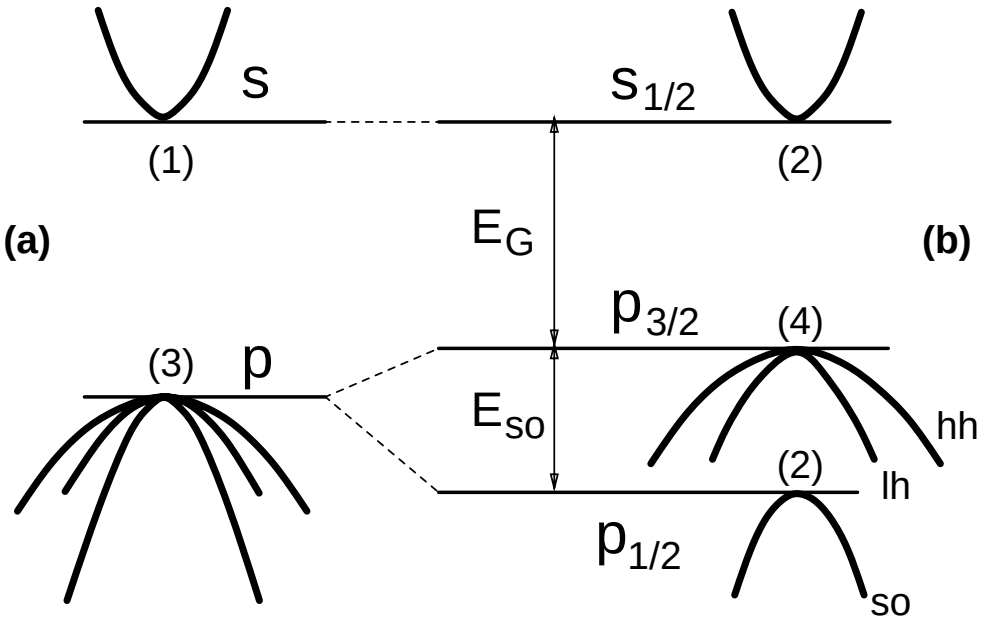

Figure 1.20. Genesis of states at the center of the Brillouin zone in cubic semiconductors. Neglecting electron spin ***(a)***, the valence band top is formed by three linear combinations of the four bonding sp^3 hybrids (cf. Fig. 1.4). These are predominantly *p* orbitals. The 4th linearly independent combination (predominantly *s*-type) is at the bottom of the valence band and is not shown in the figure. The bottom of the conduction band (in direct band semiconductors) is predominantly *s*-type, while the other antibonding hybrids (*p*-type) are in the upper range of the conduction band. Numbers in parentheses indicate the degeneracies at $\mathbf{k} = 0$. If we "include" the spin (but not the spin-orbit interaction), the degeneracies double.

Inclusion of the spin-orbit interaction ***(b)*** splits-off the two *p*-states corresponding to the total angular momentum $|jm> = |\frac{1}{2} \pm \frac{1}{2}>$. The remaining four states $|\frac{3}{2} m>$ give rise to two doubly degenerate bands, light holes ($|\frac{3}{2} \pm \frac{1}{2}>$) and heavy holes ($|\frac{3}{2} \pm \frac{3}{2}>$). The top of the valence band is $\frac{1}{3} E_{so}$ above (and top of the split-off band $\frac{2}{3} E_{so}$ below) the unperturbed valence band edge in the absence of spin-orbit coupling.

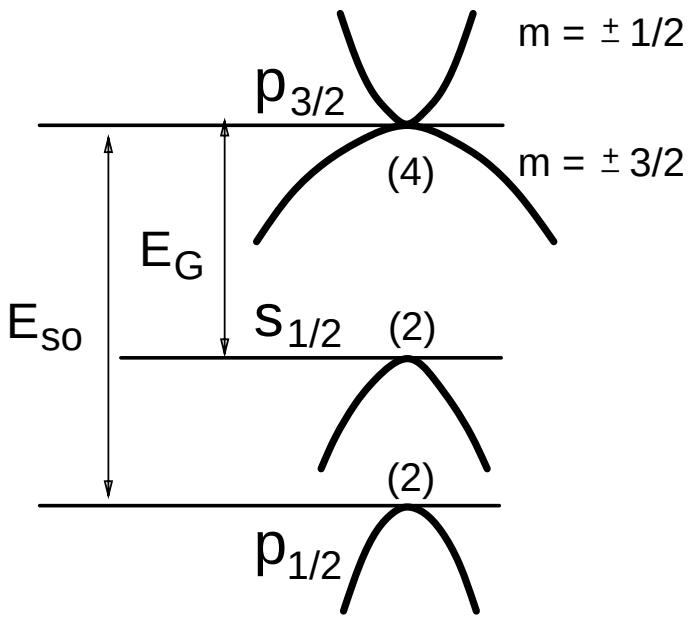

Figure 1.21. Schematic band diagram in gapless semiconductors (grey tin). In the Kane model, the gapless band structure is formally obtained by changing the sign of E_G, cf. Eq. (1.78). The $s_{1/2}$ band then becomes lower in energy than the $p_{3/2}$ band and the curvature of light-hole branch in the $p_{3/2}$ band is reversed (light holes are transformed into electrons). The bandgap is identically zero in virtue of the same symmetry that makes degenerate the light-hole and the heavy-hole branches in germanium and silicon. This symmetry can be broken by the application of a magnetic field, which leads to the emergence of a forbidden gap; similar effect can be accomplished by a uniaxial strain.

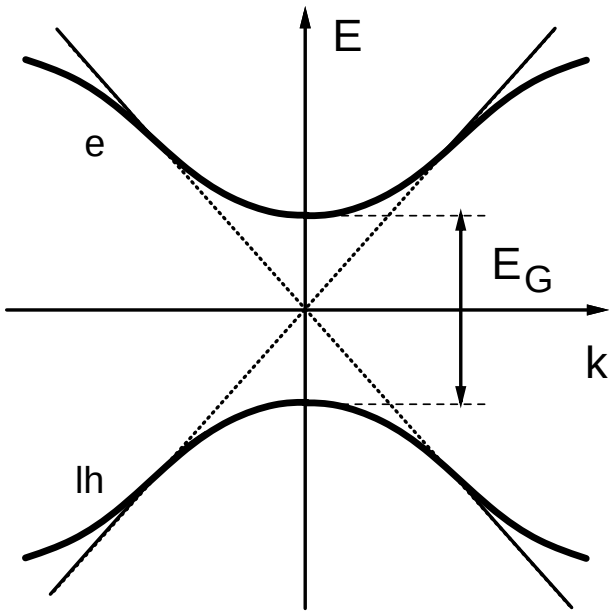

Figure 1.22. The energy-quasimomentum relation in the conduction and light-hole bands. Fat lines indicate (schematically) the exact relation, thin lines the relation given by the two band model. Slope of the dashed line gives the maximum velocity v_{max} of band electrons, which corresponds to c in the relativistic analogy. It is evident that the two-band model is approximately valid up to the inflection point on the real curve.

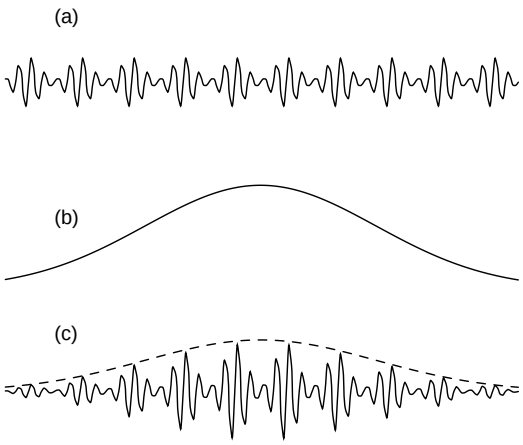

Figure 1.23. Schematic illustration of the Bloch and envelope wave functions.

(*a*) Bloch function $u(\mathbf{r})$ at $\mathbf{k}_0 = 0$ varies rapidly within the crystal unit cell.

(*b*) Envelope function $F(\mathbf{r})$ varies little on the unit cell scale.

(*c*) Complete wave function $\psi(\mathbf{r})$ of a localized electron in the effective mass approximation.